Applications of Digital Holographic Imaging at Lockheed Martin Coherent Technologies

Philip Gatt and Samuel T. Thurman
Lockheed Martin Coherent Technologies,
135 South Taylor Avenue, Louisville, CO 80027

1. Digital Holographic imaging overview

Digital holography combines the return field from a coherently illuminated object with a spatial reference laser. The angle of the reference laser is chosen to produce spatial fringes that modulate the return field sufficiently far from DC so that an image of the pupil can be extracted from the Fourier transform of the modulated data. A complex image, carrying the amplitude and phase of the image field, is extracted by inverse Fourier transforming a single sideband or pupil image (see Figure 1).

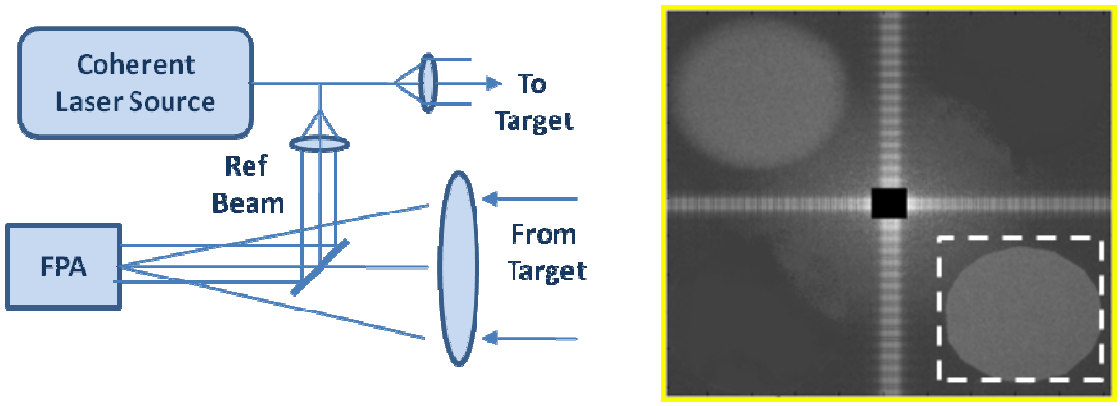

Figure 1. Digital holography experimental setup (left) and Fourier transform of the fringe modulated signal (right).

This complex demodulation process enables the direct application of many radar techniques to coherent ladar imagery, including velocity and range imaging or synthetic, inverse synthetic and multi-aperture imaging. This paper describes LMCT's advancement in these areas.

2. Range and Doppler imaging

2.1. Two-pulse velocity imaging concept

In coherent lidar, object radial velocity, V_r, is measured by estimating the Doppler shifted frequency, f_d, of the return field using the Doppler shift formula (Eq 1 left). Velocity resolution is inversely proportional to the waveform dwell time (Eq. 1 center) since frequency resolution is given by $\Delta f = 1/\Delta t$. Consequently, long dwell times are required for precision velocity estimation.

The doublet-pulse waveform has been utilized by LMCT for many years[1]. It has the advantage of being a tunable waveform facilitating a wide range of dwell times. For this waveform, velocity is measured by the estimating the phase difference between two same-frequency pulses separated in time. The velocity estimate is extracted from the phase difference, $\Delta\theta$, of the two pulses as shown in Eq. 1 (right).

$$f_d = 2V_r/\lambda \qquad \Delta V_r = \lambda/2\Delta t \qquad V_r = \frac{\Delta\theta}{4\pi}\frac{\lambda}{\Delta t}. \tag{1}$$

This phase difference represents the difference in round-trip distance, relative to a wavelength, in time Δt. This is a direct application of the Doppler shift formula, since frequency is the phase derivative ($f_d \approx \Delta\theta/2\pi\Delta t$).

2.2. Two-wavelength range imaging concept

In an entirely analogous manner to the two-pulse velocity sensing concept, two pulses separated in frequency, by bandwidth Δf can be utilized to measure the range to an object. It is well known that the range resolution is given by $\Delta R = c/2\Delta f$, where c is the speed of light. With this waveform, target range is estimated from the phase difference between the two return pulses via

$$R = \frac{\Delta\theta}{4\pi}\frac{c}{\Delta f} \tag{2}$$

The term $c/\Delta f = \lambda_1\lambda_2/|\lambda_1-\lambda_2|$ represents the synthetic wavelength corresponding to the frequency difference between the two pulses. Hence, Eq. 2 shows the range measurement is proportional to the phase, relative to a half-wave, of the synthetic wavelength.

2.3. Waveform duality principle

The duality of the range and velocity measurement techniques described above is inescapable. In fact, using the following substitutions

$$R \Leftrightarrow V,\ c \Leftrightarrow \lambda,\ \text{and}\ t \Leftrightarrow f\ , \tag{3}$$

any of the velocity expressions above can be converted to their range counterparts and vice-versa. We call this the "Waveform Duality Principle" and suggest that any valid velocity expression can be converted to a valid range expression and vice-versa using this simple concept. For example, the Cramer-Rao Lower Bound for the velocity[2] and range[3] measurement precisions of the doublet-pulse and doublet-wavelength waveforms are given by

$$\sigma_V \geq \frac{\lambda}{2\pi\sqrt{2}\Delta t}\frac{\sqrt{(1+CNR)}}{CNR} \quad \text{and} \quad \sigma_R \geq \frac{c}{2\pi\sqrt{2}\Delta f}\frac{\sqrt{(1+CNR)}}{CNR}\ , \tag{4}$$

where CNR is the waveform carrier-to-noise ratio. Obviously these two expressions are duals of each other.

2.4. Example data

In this section, we present example range and velocity imagery measured using the DH approach described above. Figure 2 (left) shows the velocity time series and corresponding amplitude spectrum extracted from many image frames at a specific location in the image of a vibrating speaker. In, Figure 2 (right) we show an image of the integrated velocity power in the 40 Hz frequency bin of the same target. This image clearly shows the portion of the speaker target that is and is not vibrating at 40 Hz.

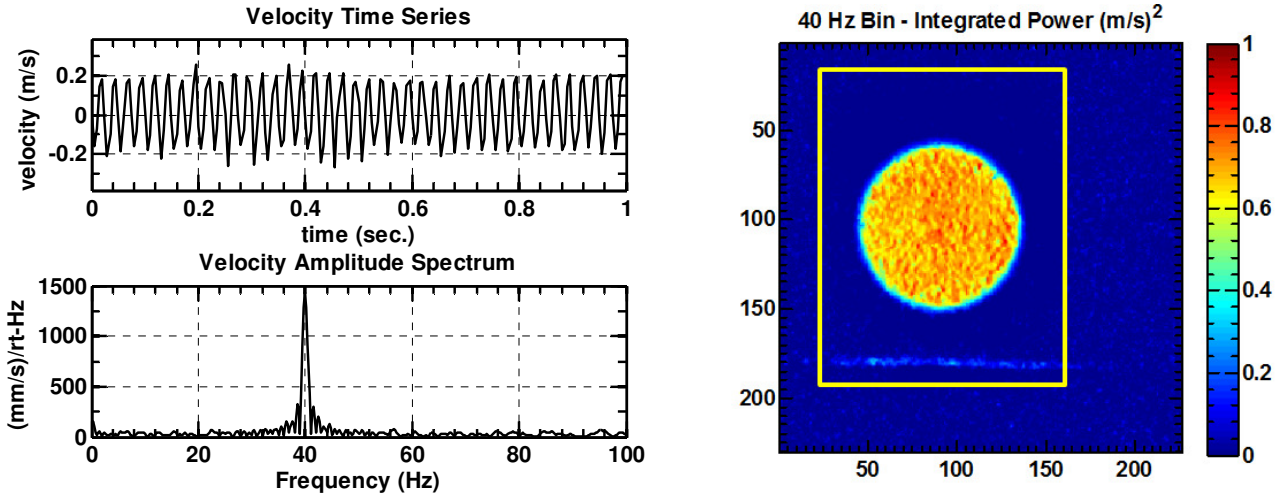

Figure 2. Speaker velocity time series and amplitude spectrum (left) and image of the spectral power at 40 Hz (right).

In Figure 3 are images of the two-wavelength interference data: amplitude (left) and unwrapped-phase difference (right) from a 3D object. The imagery in Figures 2 and 3 demonstrates the wide utility of the Digital Holography imaging approach for measuring velocity and range with the same DH hardware. Simultaneous range and velocity imaging is also feasible.

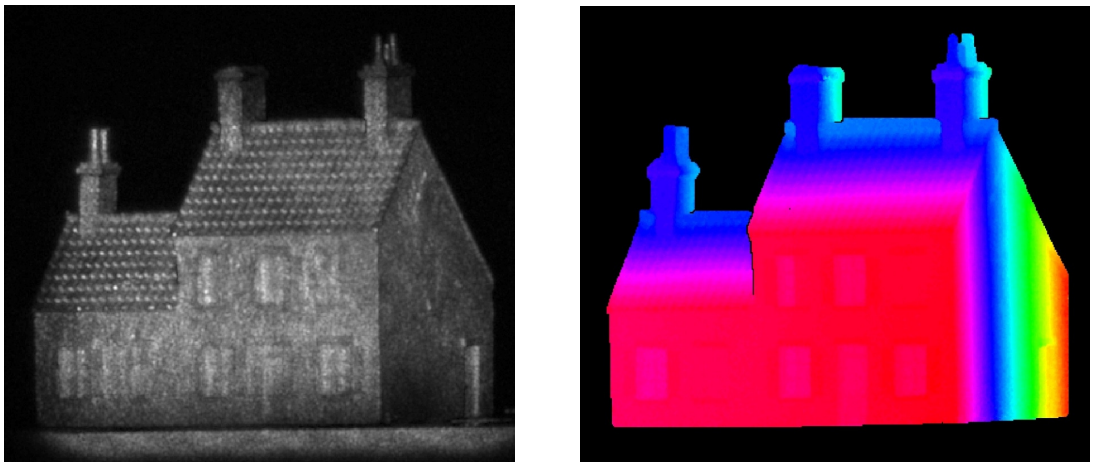

Figure 3. Two-wavelength interference amplitude (left) and unwrapped phase (right) images of the 3D object.

3. Aperture synthesis with DH imaging

3.1. Image resolution and the optical space bandwidth product

One way to think about synthetic aperture imaging resolution is in terms of object information encoded and carried by the reflected speckled field and the amount of that information that is collected by the imaging system. The space bandwidth product of the field is a measure of the field information content. The total SBP of the field can be evaluated in the target-plane as the area of the illumination beam in units of optical wavelength (Eq. 5, left). This space bandwidth product is also a measure of the number of the degrees of freedom, or speckles, of the optical field[4]. In the far field, object information is eventually evenly distributed across 2π steradians. Hence, the SBP of the field collected by the receiver pupil is given by Eq 5 (right).

$$SB_{field} \approx A_{illum} / \lambda^2 \quad \text{and} \quad SB_{pupil} \approx SB_{field} (\Omega_p / 2\pi), \tag{5}$$

where Ω_p is the solid angle subtended by the pupil at the target.

Because the SBP is conserved through propagation, the SBP of the image is equal to the SBP of the field collected by the pupil. Put another way, the number of degrees of freedom or resolution elements in the image is equal to the number of degrees of freedom or speckles collected by the entrance pupil. This is the fundamental principle behind synthetic and inverse synthetic imaging. That is, by collecting more pupil-plane speckles finer image resolution is obtained.

3.2. Synthetic and inverse synthetic aperture imaging concepts

The aim of synthetic aperture imaging is to increase receiver resolution by increasing the image SBP (number of collected speckles) by taking advantage of transmitter, receiver or target motion. This is done by tracking the speckle motion across the aperture during a data collection sequence and coherently combining all measurements to form a synthetic aperture. By acquiring more speckles worth of data than the physical receiver aperture supports, one can form a finer resolution image with a larger space bandwidth product.

3.3. Example data

Here, we present example synthetic aperture image results. Figure 4. (left) shows an image formed by averaging the intensity images obtained from 25 separate digital holograms from a single aperture. For this collection, the transmitter and receiver positions were fixed, while the target orientation was adjusted to move the reflected speckle pattern across the aperture between frames.

Figure 4 (center) shows the inverse synthetic aperture intensity image obtained by coherently combining all 25 measurements. Note that there is an inherent tradeoff between speckle reduction (diversity) and resolution improvement. The inverse synthetic aperture image sacrifices speckle diversity by using all of the available information to obtain finer spatial resolution.

Figure 4 (right) shows a multi-transmitter synthetic aperture image collected using a method described by Rabb et. al.[5] In this imaging approach a synthetic aperture is formed by illuminating the target from multiple locations

while the target and receiver are held stationary. In this example three transmitter locations at the apexes of an equilateral triangle were used to produce an image that has approximately 2X finer resolution, in each direction, than the image shown in Figure 4 (left). In this example, 25 synthetic aperture images were created (one for each target orientation) and then averaged for speckle reduction.

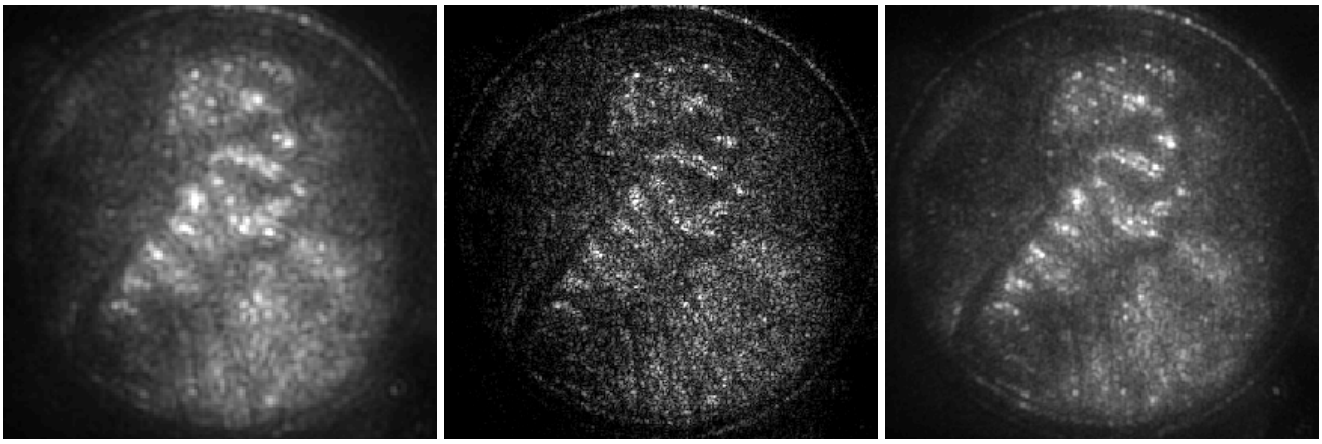

Figure 4. Incoherent average intensity image (left),
inverse synthetic aperture intensity image (center) and multi-transmitter synthetic aperture intensity image (right).

4. Summary and conclusions

In this paper we have demonstrated the wide versatility of digital holographic sensor hardware and the advancements in hardware and algorithms being developed at Lockheed Martin Coherent Technologies. We have shown that many imaging modalities are enabled by this technology that provides direct access to image amplitude and phase. These image modalities include 3D, Doppler, synthetic and inverse synthetic aperture imaging. Multi-aperture imaging is also enabled by this technology.

5. Acknowledgements

The authors acknowledge and thank the researchers whose many contributions have led to the development of this technology. In particular the authors acknowledge the contributions of Dr. Joe Marron for his vision and leadership towards the development of this technology; Dr. Van Rudd, Dr. John Glennon and Dr. Piotr Kondratko for the velocity imaging hardware, experimental work and algorithm development; Nathan Seldomridge and Andrew Bratcher for laboratory and field digital holography hardware developments and validation and demonstration experiment efforts; and Adam Villarreal for his contributions to synthetic aperture signal processing algorithms and data analysis.

6. References

[1] Hannon S M., J.A. Thomson, S.W. Henderson, P. Gatt, R. Stoneman, D.L. Bruns, “Agile Multiple Pulse Coherent Lidar for Range and Micro-Doppler Measurement,” Proceedings of the SPIE: AeroSense, V 3380, Orlando, Florida April (1998).

[2] Gatt, P. S. W. Henderson, J. A. Thomson and S. M. Hannon, “Noise Mechanisms Impacting Micro-Doppler Lidar Signals: Theory and Experiment,” Proceedings of the 2000 Military Sensing Symposia (formerly Active IRIS), Dayton, Ohio, April (2000).

[3] Gatt, P., J. Alex Thompson, and Sammy W. Henderson “Coherent Laser Radar Range Precision for Range Resolved and Unresolved Targets,” in Proc. Eleventh Biennial Coherent Laser Radar Tech. and Appl. Conference, Malvern, England (2001). [4] D. J. Rabb, D. F. Jameson, J. W. Stafford, and A. J. Stokes, "Multi-transmitter aperture synthesis," Opt. Express **18**, 24937-24945 (2010).

[4] Goodman, J. W., *Introduction to Fourier Optics,* (McGraw-Hill, New York, (1968).

[5] Rabb, D. J., D. F. Jameson, J. W. Stafford, and A. J. Stokes, "Multi-transmitter aperture synthesis," Opt. Express **18**, 24937-24945 (2010).